FINITE ELEMENT ANALYSIS OF THE SPACE TELESCOPE FOCAL PLANE STRUCTURE JOINT

W. Lee SHOEMAKER

Assistant Professor, Civil Engineering Dept., Auburn University, AL 36849

Winfred A. FOSTER, Jr.

Associate Professor, Aerospace Engineering Dept., Auburn University, AL 36849

Daniel Y. HWANG

Graduate Research Assistant, Civil Engineering Dept., Auburn University, AL 36849

Abstract

A finite element analysis of the Hubble Space Telescope focal plane structure corner joint is described. In this analysis, four three dimensional finite element models were developed to make comparisons of the element stresses calculated in the corner joint flexure plate. The models consisted of two different finite element meshes for the structural components and two different boundary conditions types - force and displacement. The loading and boundary conditions were extracted from a previous finite element model of the entire Optical Telescope Assembly.

INTRODUCTION

The Hubble Space Telescope (HST) is a general purpose high resolution astronomical observatory. As an optical instrument, the optical performance specifications required to produce an image of high quality are extremely stringent especially in the alignment of the telescope elements. Since the Space Telescope is designed to be placed in and retrieved from Earth orbit at an altitude of 590 kilometers by the Space Shuttle, it will be subjected to inertial loads during take off and landing. Hence, the structural strength, stiffness, and thermal expansion characteristics must be investigated carefully.

The major components of the HST are the Optical Telescope Assembly (OTA), Scientific Instruments (SI's), and overall Support Systems Module (SSM). The SI's are designed as modular units that can be serviced or replaced in orbit by astronauts. In the OTA, the Focal Plane Structure (FPS) is connected to the main ring which contains the Primary Mirror. The FPS houses the SI's which will convert the telescopic images into useful scientific data. The apertures of the SI's are located at the principal focus of the telescope. Hence, any parameter which affects the FPS alignment would affect the position of the SI's and reduce the accuracy of the scientific data and/or produce images of lower quality.

The four corners of the FPS are connected to the Main Ring with bipod flexure plates. Testing of the OTA has indicated a necessity to modify the flexure plate connections to the Main Ring. This modification consisted of adding titanium "boots" to increase the stiffness and strength of the flexure plate. The analysis described herein was undertaken to provide a better understanding of the load path and stress distributions in the FPS corner joints.

MSC/NASTRAN (1) was used to analyze the FPS. A finite element analysis of the entire OTA was previously performed by Lockheed Huntsville (2). While this model was adequate to study the overall behavior of the OTA, it was not intended to provide detailed analyses of specific structural components. A three dimensional finite element model of the FPS corner joint was constructed for this purpose and is the subject of this paper.

This finite element model involved complex interconnections resulting from the construction of the bolted joint. Also, the various composite materials that are used in the corner joint presented some interesting modeling challenges. This paper will describe these considerations and the effect of different types of boundary conditions that were used.

MODEL DESCRIPTION

The four connections between the HST Main Ring and the FPS are the flexure plates which are bolted to the peripheral beam, diagonal beams, and side trusses in each FPS corner joint. Graphite epoxy is the primary material for the flexure plates which also includes a unidirectional pitch layer sandwiched between two pseudo-isotropic layers. The aft end of the flexure plate transitions into a flange which is connected to the peripheral beam. Under these flanges, radius filler blocks are attached and provide additional stiffness. The primary focus of this investigation is in the area of these flexure plate flanges.

The peripheral beam is a built-up layered composite section also made of graphite epoxy. A titanium fitting rests on the aft face of the peripheral beam at each corner. This fitting is the base plate connection for two truss members that frame into the corner joint. Three 7/16" diameter steel bolts connect the fitting, peripheral beam, and flexure plate. This bolted connection was specifically designed to produce the desired load path and to prevent unwanted thermal growth between components. Shear forces between the truss fitting and the peripheral beam in the V2-V3 plane are transmitted through shear cones at the interface as shown in Figure 1. These shear cones bear on composite wound bushings that are fitted through the

peripheral beam providing a gap between the bottom of the truss fitting and the aft face of the peripheral beam. Any axial forces in the truss members which put the sandwiched joint in compression are transmitted through the shear cone, bushing, and aft flange of the flexure plate. However, any axial forces which apply tension to the joint are transmitted between the truss fitting and the aft flange of the flexure plate directly through the bolts. Moreover, there are an additional seven 7/16" diameter and one 1/2" diameter steel bolts, connecting the peripheral beam to the aft flange of the flexure plate. These bolts provide shear transfer in the V2-V3 plane between the peripheral beam and the flexure plate. The 7/16" diameter steel bolts are countersunk into the aft side of the peripheral beam so that they will not interfere with the truss fitting. The three through-bolts previously mentioned are loose fitting inside the peripheral beam bushing and do not transmit shear at the peripheral beam/flexure plate interface. This interface is bonded only by the pre-compression applied through the bolts and friction.

FINITE ELEMENT MODEL DESCRIPTION

MESH DESCRIPTION

There are a total of 2238 elements, 2935 nodes, and 9297 degrees of freedom in the model of the corner joint. Both two- and three- dimensional elements were used on the

model. The element types used for each component of this model are summarized in Table 1. The MSC/NASTRAN (1) tetrahedron (TETRA), hexahedron (HEXA), and pentahedron (PENTA) elements are all solid elements. Mid-side nodes were used on 36 of the hexahedron elements of the peripheral beam model in order to match locations of the connected bolts.

Flexure Plate Mesh

The flexure plate is made of three sandwiched components which includes outer layers of pseudo-isotropic graphite epoxy material (GY-70) and an inner core of unidirectional composite material (P-75S). Each of the three layers were subdivided into two solid elements through the thickness. The inner unidirectional layer tapers off at the top and bottom of the flexure plate. Therefore, the six solid elements transition into four solid elements at these tapers. The titanium boots were modeled with one layer of solid elements on the sides of each leg of the flexure plate. A 3-D view of the entire flexure plate model is shown in Figure 2.

Peripheral Beam and Deck Mesh

The peripheral beam is a built-up layered structure made of twelve pseudo-isotropic composite layers (P-75). Because the layers are isotropic in the plane of each layer and the fibers of the layers have the same orientation,

there is no need to represent each layer with finite elements. Three layers of solid elements were used to model the cross-section of the peripheral beam. Figure 3 shows a three dimensional view of the peripheral beam. The actual peripheral beam transitions into an I-shape at the midsides. However, the finite element model of the peripheral beam which extends into this midside zone still represents the cross-section as rectangular. The stiffness of this portion is modified to reflect the stiffness of the I section. This is done with an equivalent modulus of elasticity.

The deck plate was modeled with QUAD4 and TRIA3 elements as shown in Figure 3. The deck plate has a cut out for a fitting to attach to the diagonal beam. The deck plate elements are connected to the inner face of the peripheral beam between the second and third solid elements representing the peripheral beam cross-section.

Diagonal Beam Mesh

The diagonal beam used in this model was extracted from the Lockheed model. Since only the stiffness of the diagonal beam was required to evaluate the stresses in the flexure plate, a coarse mesh which simplified the built-up diagonal beam was used. However, this diagonal beam model did not match the new corner joint model and tended to yield poor results. This first model will be referred to as the Original Model. A more refined mesh for this interface was generated and compared with the coarse mesh. This

comparison is shown in the next section. The modified diagonal beam was composed of QUAD4 and TRIA3 elements. A 3-D view of the diagonal beam is shown in Figure 4.

BOUNDARY CONDITIONS AND LOADS

Intra-model Connections

The modeling of the connections between the three components of the FPS corner joint (flexure plate, peripheral beam and diagonal beam) emphasized simulating the load paths provided by the actual connection (3,4) as opposed to a stress distribution model. Figure 5 shows the assembled components in a three dimensional view.

Flexure Plate - Peripheral Beam Interface. The connection of the peripheral beam to the flexure plate including the side truss foot was modeled using uniaxial elements and imposed displacement conditions between the components. A diagram showing the bolt pattern and mesh overlay of the peripheral beam and upper flange of the flexure plate is shown in Figure 6. These meshes do not coincide except for specific nodes required for the interface. The fine mesh needed to match the geometry in the area of concern on the upper flange of the flexure plate was not needed to model the peripheral beam. The points A-K where bolts are located and the points labeled 1-6 which are not bolt locations have coincident nodes on both the flexure plate and peripheral beam as shown on Figure 6. The

connections between these coincident nodes are defined in Table 2. The displacement constraints listed in Table 2 provide shear transfer in the X-Z plane at the peripheral beam/flexure plate interface at bolts labeled D-K on Figure 6. Bolts A-C do not transmit shear due to their loose fit in the composite wound bushing. All of the 17 coincident node sets on this interface are connected in the Y direction as noted in Table 2.

The composite wound bushings and three side truss footing bolts are located at A, B and C on Figure 6. Three independent nodes on top of the peripheral beam were defined with the same coordinate to allow for the effect of the shear cones. These nodes are connected to the corresponding nodes on the peripheral beam in the X and Z directions. This allows shear transfer in the X-Z plane corresponding to the action of the shear cone. The bushings are attached to these three independent nodes and the corresponding nodes at the bottom of the peripheral beam. The three bolts are attached between these same nodes and the corresponding nodes on the bottom of the radius filler. The three independent nodes are also connected to node 70205 which is located where the line of action of the side truss members intersects the peripheral beam by displacement constraints in the X, Y, and Z directions.

The nodal forces at node 70205 from the Lockheed model are then applied and transferred proportionately to the

three independent nodes to simulate the load transfer through the side truss into the three bolts. The other eight bolts connect the peripheral beam to the flexure plate. All of these bolts connect the corresponding node at the upper node of the peripheral beam and the lower node of the radius filler block.

A preload of 6500 pounds in all 11 bolts was introduced using a thermal gradient to pre-shrink the bolts and produce the required effect.

Inter-model Boundary Conditions

There are three different boundary conditions utilized in this model. Each case will be described in this section.

For boundary condition-I, which will be called "Modified Model-I", the force boundary conditions were used in the 3-D model. The flexure feet which attach to the main ring were assumed fixed. All nodes at the bottom surface of the feet were restrained in all degrees of freedom. The other boundaries which include the cross-section of the peripheral beam, the cross-section of the diagonal beam, and the side truss were all modeled using force boundary conditions taken from the Lockheed model.

For boundary condition-II which will be called "Modified Model-II", the bottom of the flexure feet were still assumed fixed as before. However, displacement boundary conditions taken from the Lockheed model were applied to the peripheral beam and diagonal beam.

Boundary condition-III which will be called "Modified Model-III", was the same as Modified Model-II except displacement boundary conditions were also applied to the flexure feet instead of them being fixed.

RESULTS AND COMPARISON

In this investigation, two load cases obtained from Marshall Space Flight Center were applied to this model with three kinds of boundary conditions. These two loading cases were also used earlier in the Lockheed model analysis.

The models discussed here can be classified as:

1. ORIGINAL MODEL (5): A FEM model with coarse mesh of the interfaces of the three components (flexure plate, peripheral beam, and diagonal beam) was used. The flexure feet attached to the main ring were assumed fixed. The cross-section of peripheral beam and diagonal beam were released but with boundary forces taken from Lockheed model.
2. MODIFIED MODEL-I (6): A FEM model the same as the original model except the interfaces of the three components were modified with a more refined mesh. The flexure feet were still assumed fixed and the force boundary conditions used were the same as original model.
3. MODIFIED MODEL-II (6): A FEM model with the same

geometry as Model-I. The flexure feet were still assumed fixed here but displacement boundary conditions were added at the boundaries of peripheral beams and diagonal beam.

4. MODIFIED MODEL-III (6): A FEM model with the same geometry as Model-I. The boundary conditions used were the same as Model-II except the flexure feet were released and given displacement and force boundary conditions.

After analyzing the FEM models, the element stresses were carefully scanned to determine whether any stresses in the flexure plate exceeded the allowable stresses. The allowable stresses are based on a factor of safety of 2.25 on the appropriate ultimate strength of the material.

Because the upper flange of the flexure plate is the focus of this investigation, the maximum principal in-plane normal stresses and shear stress of the outside layer elements shown in the shaded area in Figure 7 were calculated. When calculating the principal stresses, the effects of the shear stresses in the element Z-direction were ignored. A check of several elements showed that this simplification resulted in less than 5% difference in the principal stress considering all of the stress components. The results of the principal stresses are summarized in Table 3 and Table 4.

After comparing the results from the Original Model and the Modified Model-I for the Liftoff Case No.1, it was found that the modified elements stresses of concern were about 50% of those from the original. Thus, using a more refined mesh at the component interface, all of the stresses (except in elements adjacent to preloaded bolts) in the upper flange of the flexure plate and in the flexure legs were within the allowable limits for this load case. However, for Landing Load Case No.21, higher stresses were found in the upper flange of Modified Model-I than occurred in the Original Model. In this area, the ratio of the stresses in the Modified Model-I to the stresses in the Original Model ranged from 0.8 to 2.5. The element stresses in the flexure legs remained about the same for this load case, ranging from 0.8 to 1.2.

The use of displacement boundary conditions instead of force boundary conditions as in Modified Model-II and Modified Model-III produced quite different results. The resulting displacements obtained when using force boundary conditions were generally two orders of magnitude larger than the actual displacements from the Lockheed model. The element stresses in both of these models were very similar and all lower than the allowable stresses for these two load cases.

CONCLUSION AND SUMMARY

A 3-dimensional finite element model (Original Model) of the FPS corner joint was developed (5) which provided more detail regarding the stress distribution than was previously available (2).

The modified finite element model of the FPS corner joint presented in this study reflects a more refined connection of the three components (flexure plate, peripheral beam, and diagonal beam). This modified model employed three different boundary conditions to evaluate the stresses in the upper flange of the flexure plate and were compared to the Original Model.

The modified model, with very precise interfaces that eliminated the local stress concentrations due to coarse interfaces in the Original Model, provided a more accurate stress distribution in the upper flange of the flexure plate as well as in the flexure legs.

Three kinds of boundary conditions were compared in this modified model to determine which were more suitable based on the information available from the finite element model of the entire OTA (2). After checking the results, we found that the element stresses were reduced considerably whenever the model was accompanied with displacement boundary conditions such as Modified Model-II and Modified Model-III.

The boundary conditions for these precise 3-D FEM models were taken from the Lockheed model - a quite coarse model of the entire OTA. Ideally, the use of either forces or displacements as boundary conditions should produce identical results (7,8). However, when the boundary of the model does not exactly match the location of nodes on the model from which the forces or displacements are being extracted, some problems are presented. In particular, the force distribution will have to be approximated when used as an input boundary condition. Also the overall stiffness of the more refined model will differ from the coarse model and the resulting displacements will differ from the displacements in the coarse model when the force boundary conditions are applied.

Using displacement boundary conditions, on the other hand, insures that the refined model will have the same displacements at the matching nodes on the boundary. Boundary nodes in between imposed displacements will conform based on the structural stiffness. This will maintain overall compatibility with the coarse model.

The use of boundary conditions from a coarse model onto a more refined substructure offers a method to evaluate stresses in regions of concern without requiring a fine mesh or transitional meshes on large complex structures. However, this study indicates that although force boundary conditions should theoretically yield comparable results,

displacement boundary conditions insure overall compatibility with the "parent" mesh. Assuming that the coarse analysis is sufficient to accurately produce key displacements, the use of displacement boundary conditions is a more reliable approach. It is noted that the parent model might be used in an exact zooming method (9) to eliminate some of approximations used in the application of displacement boundary conditions to nodes on the refined method.

Using displacement boundary conditions and the improved interface between components, the stresses in the areas of concern were within allowable limits for the two load cases analyzed.

ACKNOWLEDGEMENTS

This work was in part supported by the George C. Marshall Space Flight Center (MSFC) under NASA contract No. NAS8-36288. In particular the authors are most grateful to Mr. Gwyn Faile, NASA Project Coordinator, for his efforts in providing data for this research.

Table 1. Element Summary

COMPONENT	No. of ROD	No. of TETRA	No. of HEXA	No. of PENTA	No. of QUAD4	No. of TRIA3
Flexure Plate	--	3	1476	242	--	--
Boots	--	--	96	--	--	--
Diagonal Beam	--	--	--	--	39	182
Peripheral Beam	--	--	114	12	--	--
Deck Plate	--	--	--	--	18	22
Bracket	--	--	--	--	12	8
Bolts	11	--	--	--	--	--
Bushings	3	--	--	--	--	--
Total	14	3	1686	254	69	212

Table 2. Flexure Plate-Peripheral Beam Interface Multi-Point Constraints

Label in Figure 6	Flexure Plate Node	Peripheral Beam Node	Connected DOF's
1	106062	303204	Y
2	106058	303202	Y
3	106054	303200	Y
4	106040	303218	Y
5	106028	303210	Y
6	107060	303244	Y
A	106038	303216	Y
B	106034	303214	Y
C	107058	303243	Y
D	106036	303215	X,Y,Z
E	106032	303213	X,Y,Z
F	106030	303212	X,Y,Z
G	107066	303247	X,Y,Z
H	107064	303246	X,Y,Z
I	107062	303245	X,Y,Z
J	107056	303242	X,Y,Z
K	107054	303241	X,Y,Z

Table 3. Principal Stresses in the Corner for Liftoff Case No.1

Principal Stresses	Max. Stress		Min. Stress		Max. Shear
	from	to	from	to	
ORIGINAL MODEL	-6.71	6.69	-11.94	0.79	4.80
MODEL - I	-2.01	3.99	-4.57	1.11	2.29
MODEL - II	-1.29	3.82	-3.82	0.93	1.88
MODEL - III	-1.06	3.76	-3.12	1.00	2.21

Table 4. Principal Stresses in the Corner for Landing Case No.21

Principal Stresses	Max. Stress		Min. Stress		Max. Shear
	from	to	from	to	
ORIGINAL MODEL	-1.69	13.33	-9.78	3.76	11.56
MODEL - I	-3.27	15.28	-13.72	1.58	7.24
MODEL - II	-1.20	3.24	-4.29	1.00	2.14
MODEL - III	-2.33	4.47	-3.32	1.63	2.11

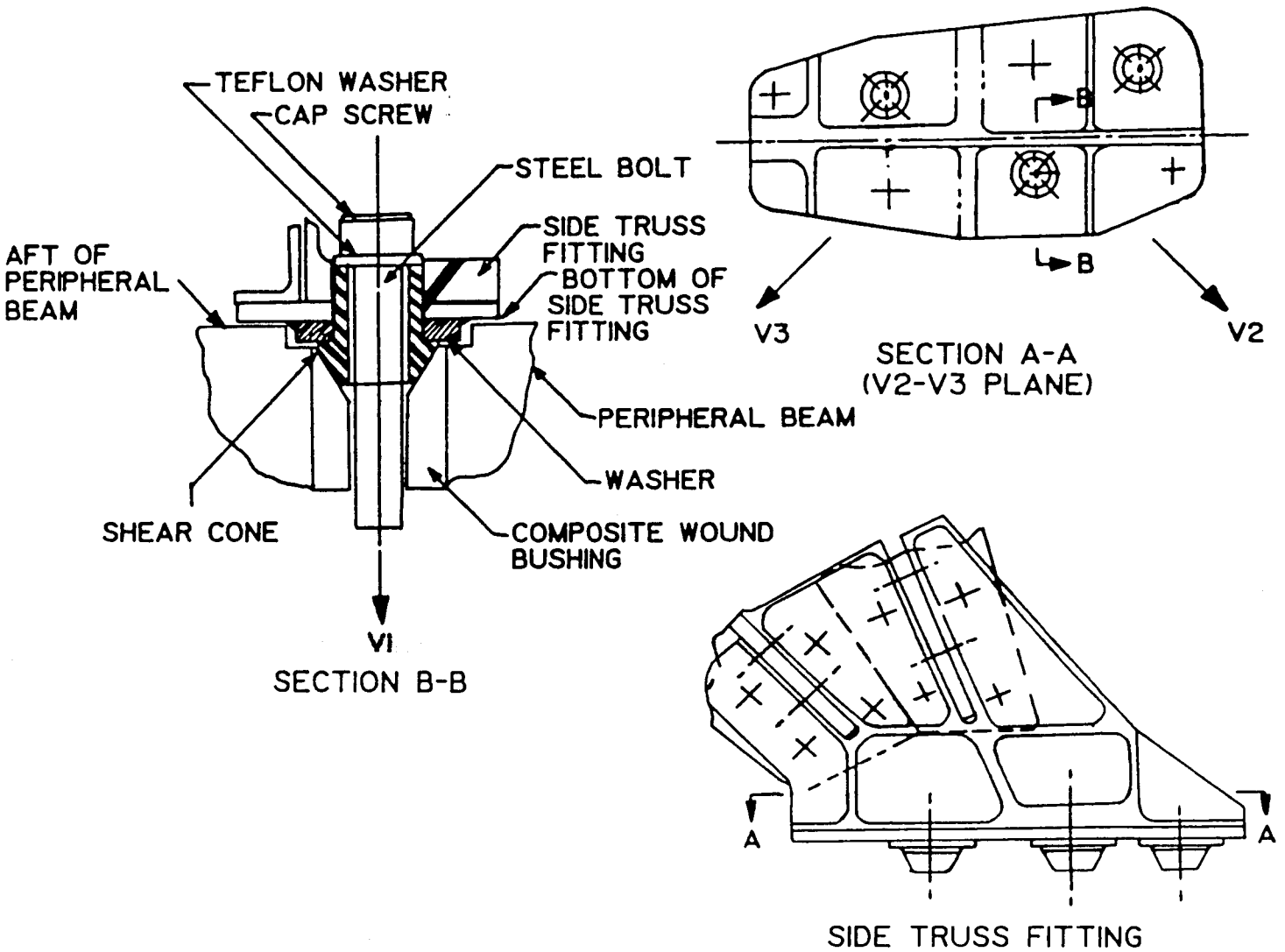

Figure 1. Side Truss Foot (Fitting) and Shear Cones

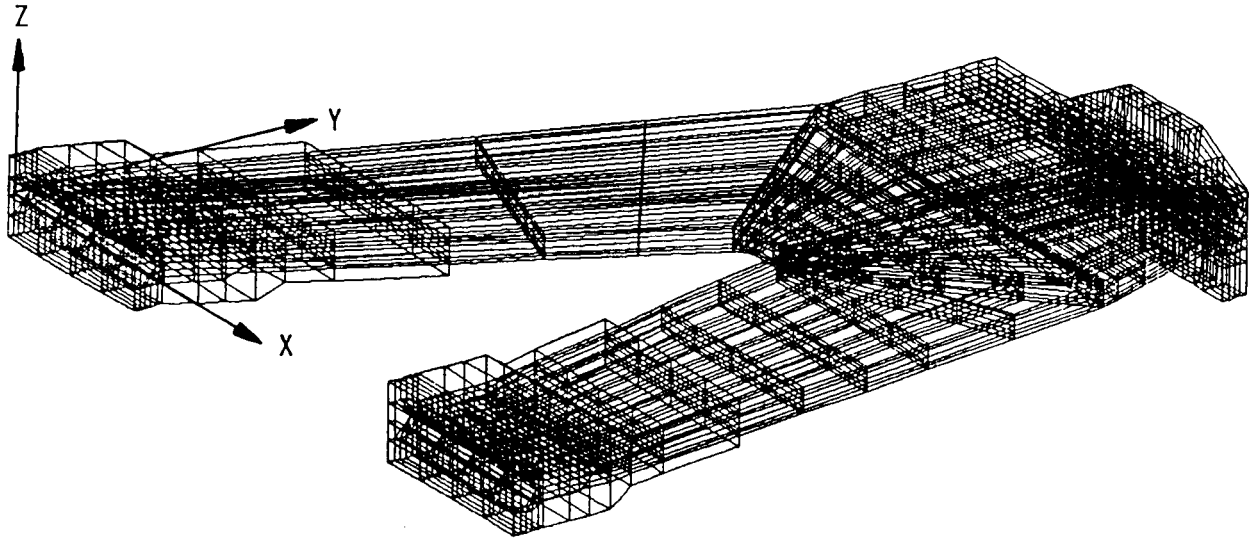

Figure 2. 3-D View of Flexure Plate Model

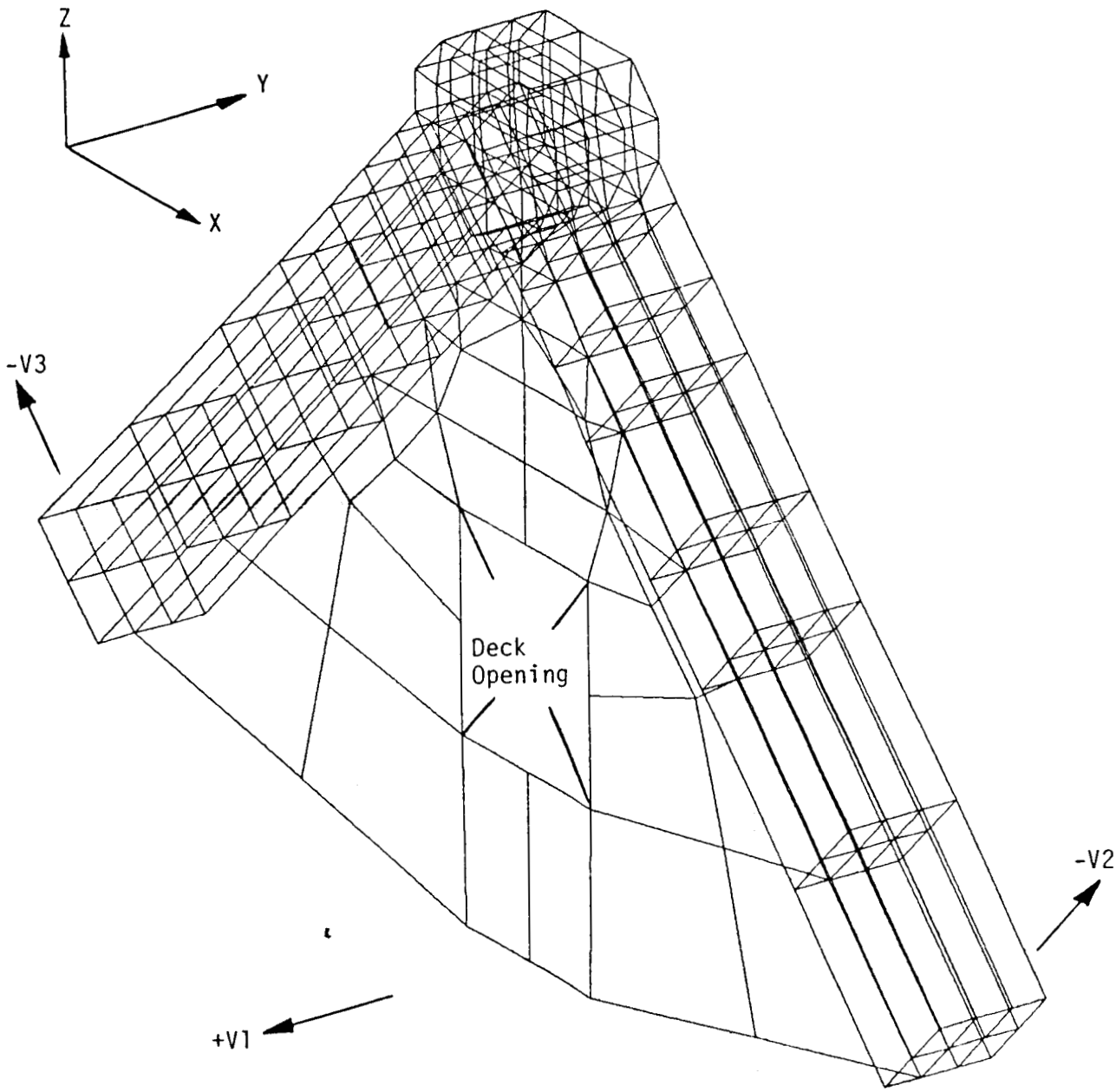

Figure 3. 3-D View of Peripheral Beam and Deck Plate Model

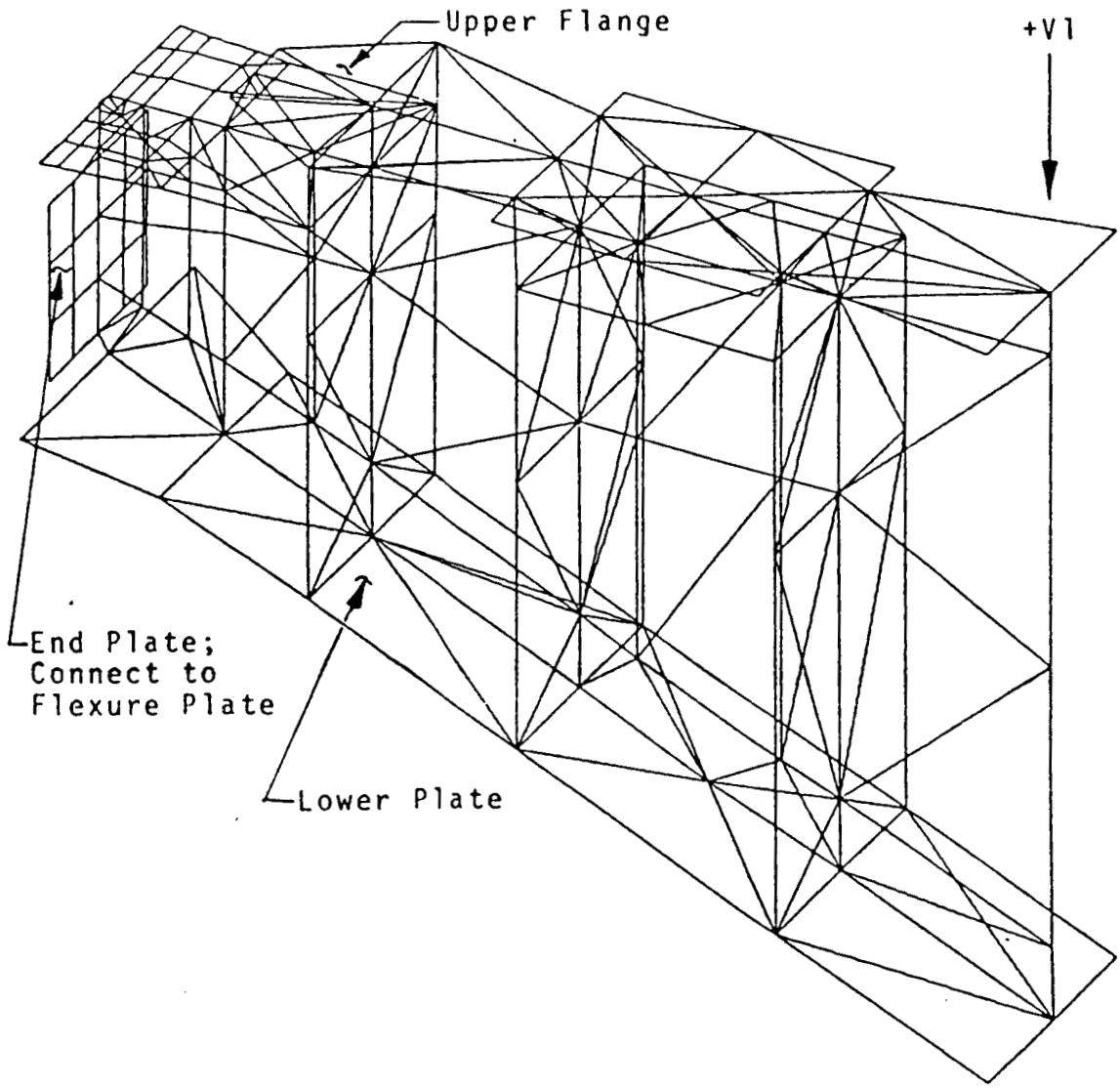

Figure 4. 3-D View of Diagonal Beam Model

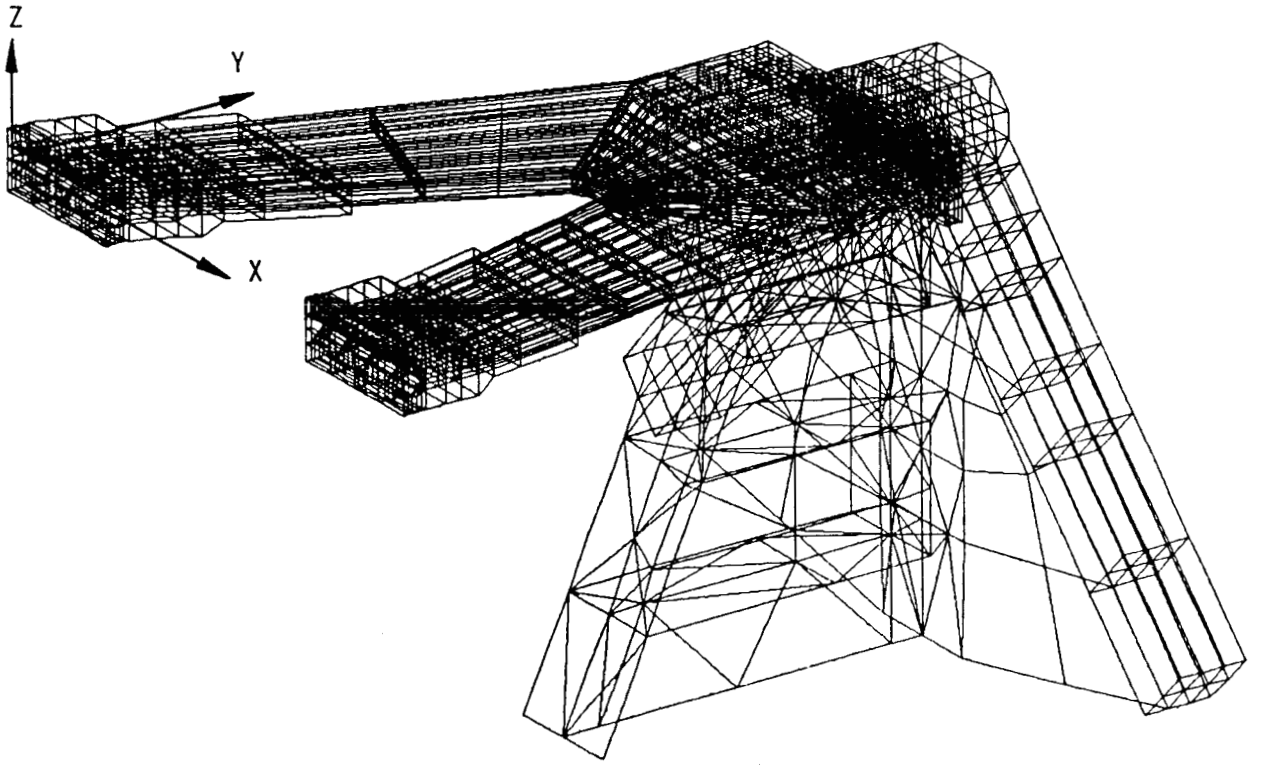

Figure 5. 3-D View of Entire FPS Corner Joint

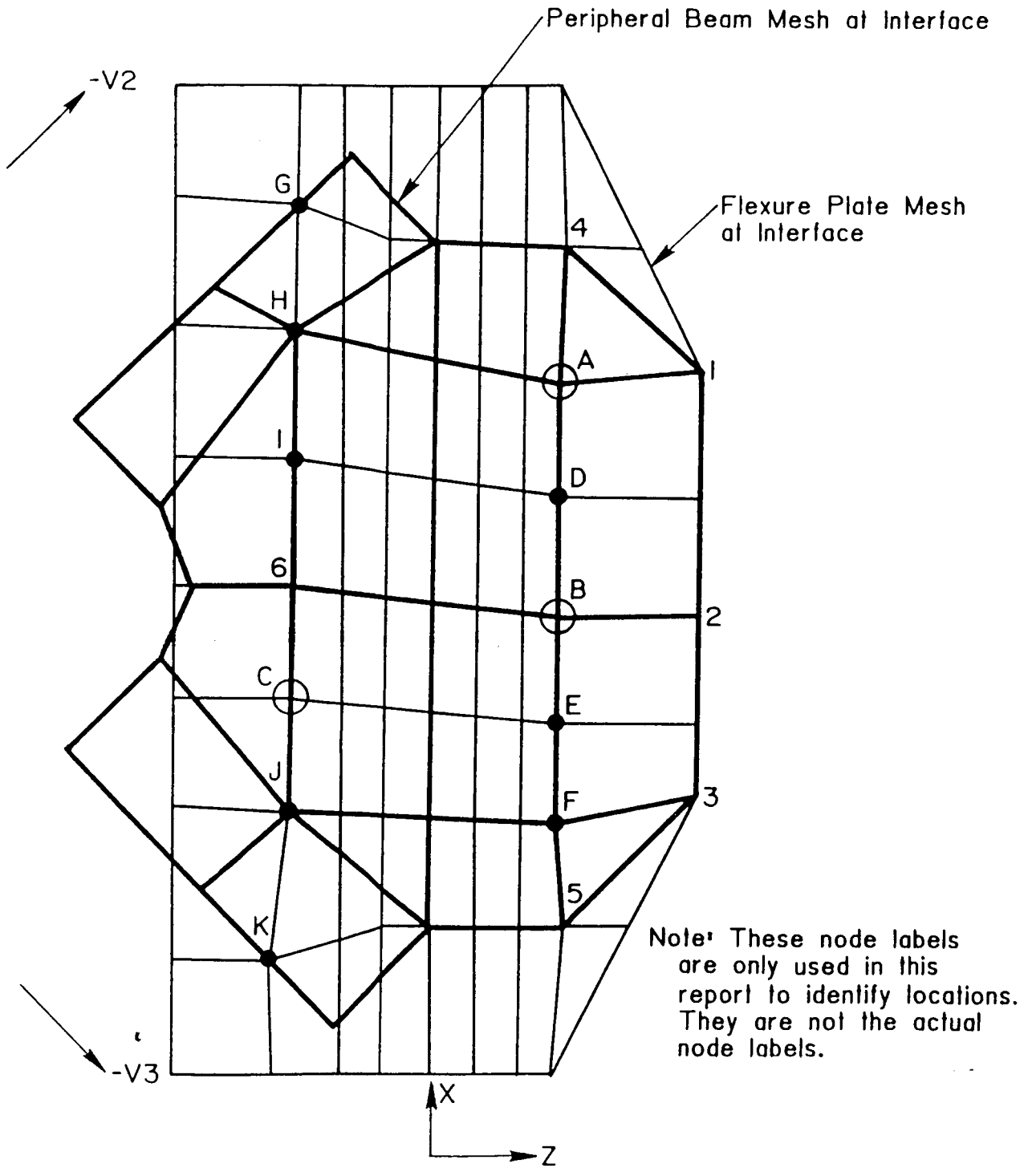

Figure 6. Key Diagram to Peripheral Beam/Flexure Plate Interface Nodes

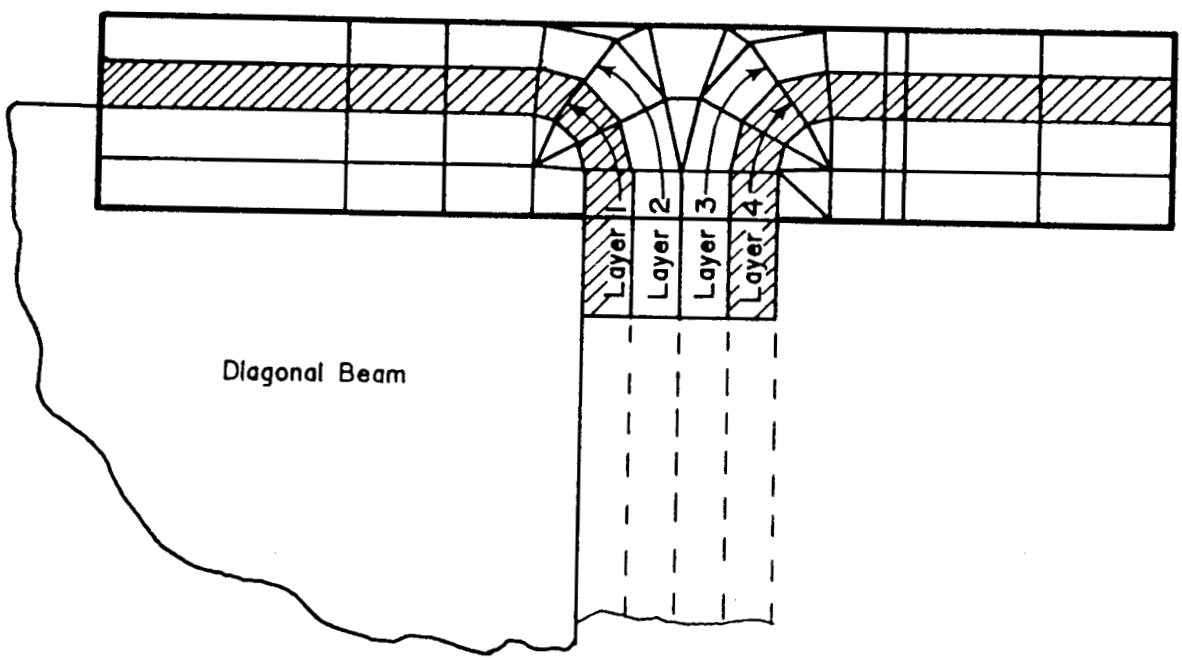

Figure 7. Side View of Flexure Plate Upper Flange

Analysis", McGraw-Hill, New York, 1968.

(9) I. Hirai, Y. Uchiyama, Y. Mizuta, and W. D. Pilkey, "An Exact Zooming Method", Finite Elements in Analysis and Design, Vol. 1, No. 1, pp. 61-69, 1985.

REFERENCES

(1) "MSC/NASTRAN User's Manual", Version 64, The Macneal Schwendler Corporation, Los Angeles, California, 1984.

(2) "Optical Telescope Assemby Analysis", Lockheed Huntsville Research and Engineering Center Technical Report D697999, Huntsville, Alabama.

(3) Santosh K. Arya, and Gilbert A. Hegemier, "Finite Element Method for Interface Problems", ASCE J. Struct. Div., Vol. 108, No. ST2, pp. 327-342, 1982.

(4) John L. Bretl, and Robert D. Cook, "Modelling the Load Transfer in Threaded Connections by the Finite Element Method", Int. J. Numerical Methods in Eng., Vol. 14, No. 9, pp. 1359-1377, 1979.

(5) **Winfred A. Foster, Jr.**, and W. Lee Shoemaker, "Stress Analysis of the Space Telescope Focal Plane Structure Joint", Auburn University Engineering Experiment Station Report, No. NAS8-36288, Auburn, Alabama (1986).

(6) Daniel Y. Hwang, "Finite Element Analysis of the Space Telescope Focal Plane Structure Joint", M.S. Thesis in Civil Engineering Dept., Auburn University, Auburn, Alabama (1987).

(7) J. S. Przemieniecki, "Matrix Structural Analysis of Substructures", AIAA J. Vol. 1, No. 1, pp. 138-147, 1963.

(8) J. S. Przemieniecki, "Theory of Matrix Structural